

A turanose-insensitive mutant suggests a role for *WOX5* in auxin homeostasis in *Arabidopsis thaliana*

Silvia Gonzali^{1,†}, Giacomo Novi^{1,†}, Elena Loreti², Fabio Paolicchi¹, Alessandra Poggi¹, Amedeo Alpi¹ and Pierdomenico Perata^{3,*}

¹Department of Crop Plant Biology, University of Pisa, Via Mariscoglio 34, Pisa, Italy,

²Institute of Biology and Agricultural Biotechnology, CNR, Via del Borghetto 80, 56124, Pisa, Italy, and

³Sant'Anna School of Advanced Studies, Piazza Martiri della Libertà 33, 56127 Pisa, Italy

Received 15 April 2005; revised 4 July 2005; accepted 23 August 2005.

*For correspondence (fax +39 0502 216532; e-mail p.perata@sss.it).

†These authors equally contributed to this work.

Summary

Sugars acting as signalling molecules regulate many developmental processes in plants, including lateral and adventitious root production. Turanose, a non-metabolizable sucrose analogue, profoundly affects the growth pattern of *Arabidopsis* seedlings. Turanose-treated seedlings are characterized by a very short primary root and a short hypocotyl showing the production of adventitious roots. A *turanose-insensitive* (*tin*) mutant was identified and characterized. Because of a T-DNA insertion and a chromosomal translocation, *tin* expresses a chimeric form of *WOX5*, a gene known to be expressed in the root quiescent centre. The *tin* mutation can be complemented by overexpression of *WOX5*, suggesting it is a loss-of-function mutant. We found that *WOX5* is both turanose- and auxin-inducible. Moreover, turanose insensitivity is associated with altered auxin homeostasis, as demonstrated by the constitutive activation of indole acetic acid (IAA) conjugation and *SUPERROOT2* expression in *tin*. On the basis of turanose effects on wild-type seedlings and the *tin* molecular and hormonal phenotype, we propose a role for *WOX5* in the root apical meristem as a negative trigger of IAA homeostatic mechanisms allowing the maintenance of a restricted area of auxin maximum, which is required for a correct root-formation pattern.

Keywords: *Arabidopsis*, auxin, root, sugar sensing, turanose, *WOX5*.

Introduction

The root system is of primary importance for providing plant anchorage to the soil, for water uptake and for plant nutrition. A wide root network allows the plant to explore the soil and facilitates extraction of mineral nutrients; growth of lateral roots contributes to improving the overall efficiency of the plant (Casimiro *et al.*, 2003). The development of lateral roots involves some of the root pericycle cells that, as a consequence of still largely unknown triggers, re-enter the cell cycle, leading to a well defined programme of oriented cell divisions to produce a lateral root primordium that will develop a meristem at the tip, growing as a mature root (Malamy and Ryan, 2001; Vanneste *et al.*, 2005).

Auxin is required for the production of lateral roots (reviewed by Casimiro *et al.*, 2003; Casson and Lindsey, 2003; Vanneste *et al.*, 2005). Mutants with altered auxin homeostasis, *superroot1* (*sur1*, Boerjan *et al.*, 1995) and

superroot2 (*sur2*, Delarue *et al.*, 1998), show increased lateral root production and several adventitious roots originating from the hypocotyl. This is due to elevated auxin levels resulting from their inability to redirect the flow of auxin precursors to the synthesis of indole glucosinolates rather than to auxin (Barlier *et al.*, 2000; Mikkelsen *et al.*, 2004).

Sugars play a role in plant development and physiology. Embryogenesis, seed germination, and seedling and tuber development are processes profoundly influenced by sugars, often interacting with phytohormones (Gibson, 2005; Koch, 2004). Glucose affects hypocotyl elongation and greening of cotyledons (Gibson, 2005; Jang *et al.*, 1997); trehalose inhibits root elongation (Wingler *et al.*, 2000); and a high sucrose:nitrogen ratio represses lateral root initiation (Malamy and Ryan, 2001). The inhibition of lateral root

production is accompanied by an increase in auxin content in the hypocotyl, suggesting that sucrose may inhibit auxin translocation to the root system (Malamy, 2005). Sucrose, fructose and glucose stimulate the formation of adventitious roots when applied exogenously in direct contact with the hypocotyl (Takahashi *et al.*, 2003). A mutant showing a sucrose-conditional defect in the patterning of distal elements in the lateral root meristem has been described recently by Horiguchi *et al.* (2003). These results indicate that sugars can affect the development of lateral and adventitious roots.

It is not easy to assess the role of sugars in plant development, a consequence of their dual role as metabolites and signalling molecules. The use of non-metabolizable sugar analogues such as palatinose and turanose allow uncoupling of the metabolic role of sugars from their signalling function. Sucrose, palatinose and turanose possess a glucose moiety linked to fructose, but differ from one another in the chemical link position (1 → 2, 1 → 6 and 1 → 3, respectively). Palatinose is not recognized by sucrose transporter(s) and does not compete for sucrose transport (Li *et al.*, 1994; M'Batchi and Delrot, 1988; Schmitt *et al.*, 1984); and the ability of the Arabidopsis SUT1 transporter to recognize turanose has been reported (Chandran *et al.*, 2003). Turanose and palatinose have been used successfully to dissect the sucrose-signalling pathway in plants (Ferne *et al.*, 2001; Loreti *et al.*, 2000; Sinha *et al.*, 2002).

In order to improve understanding of the role of sugars in root development, we studied the effects of turanose on Arabidopsis seedlings. Turanose-treated seedlings show a very short root and produce adventitious roots on the hypocotyl. Here we describe a *turanose-insensitive* (*tin*) mutant. Cloning of the *TIN* gene suggests a role for the *WOX5* gene in root development.

Results

Identification of a turanose-insensitive mutant

The rapid metabolism of sucrose into its constituent hexoses hampers easy approaches to sucrose sensing (Loreti *et al.*, 2000). We used the non-metabolizable sucrose analogues palatinose and turanose to establish the ability of Arabidopsis seedlings to sense disaccharides. Seeds were germinated on Murashige–Skoog (MS) medium in the absence of added sugars, or supplemented since imbibition with 90 mM sucrose, turanose, palatinose or mannitol as an osmotic control. Seed germination was not affected by these treatments. Sucrose promoted the growth of both root and hypocotyl, while palatinose and mannitol promoted root growth slightly (Figure 1a,b). On the contrary, both hypocotyl (Figure 1a) and root growth (Figure 1b) were reduced by turanose, and these effects were reverted by the addition of 15 mM sucrose (data not shown). Mutants and

transgenics with altered sugar sensing or metabolism did not rescue Arabidopsis seedlings from turanose inhibition of growth (Figure S1).

We screened a collection of T-DNA-tagged mutants, searching for a turanose-insensitive phenotype. This was identified and named *tin*. Turanose-treated wild-type seedlings were small, with a short hypocotyl and a very short root (Figure 1c). The *tin* mutant was slightly shorter than the wild type when grown on the control medium, but maintained normal root and hypocotyl growth on turanose (Figure 1c). Turanose mimics sucrose in its ability to stimulate adventitious roots on wild-type hypocotyls (Figure 1d,e). In the *tin* mutant the number of adventitious roots induced by turanose and sucrose was clearly lower (Figure 1d–f). Adult *tin* plants did not show any apparent morphological differences from the wild type, but their flowering time was delayed due to a prolonged vegetative phase, as demonstrated by a higher number of rosette leaves at the time of bolting (data not shown).

The gravitropic response was altered in wild-type seedlings, but not in *tin* mutant seedlings grown on turanose-containing vertical agar plates (Figure 1g). This result suggests that turanose alters the physiology of the plant hormones involved, namely ethylene and auxin.

Turanose induces ethylene production

With the aim of verifying the effects of sugars on ethylene levels, gas samples were taken from vessels containing seedlings treated with sucrose or turanose, and analysed by gas chromatography for ethylene content. Turanose treatment enhanced ethylene production in wild-type seedlings and a modest effect of sucrose was also detected (Figure 2a). *tin* overproduced ethylene on the control medium; and sucrose, but not turanose, enhanced ethylene production (Figure 2a). The wild type was shown to be sensitive to 1-aminocyclopropane-1-carboxylic acid (ACC), an ethylene precursor, as demonstrated by the lower lengths of hypocotyl and root exhibited by seedlings grown on MS medium containing ACC, while insensitivity was observed, as expected, in the ethylene-insensitive *etr1-3* mutant (Figure 2b). The behaviour of the *tin* mutant was intermediate (Figure 2b), suggesting that ethylene may play a role in the effects of turanose on root and hypocotyl growth. This hypothesis was, however, ruled out as none of the mutants defective in ethylene sensing that were tested (*etr1-1*, *etr1-3*, *ein2*, *ein2-1*) displayed insensitivity to turanose (Figure 2c).

tin mutant shows altered auxin physiology

The phenotype of turanose-treated seedlings, showing enhanced adventitious roots, suggests that the level of auxin might be elevated as a consequence of exposure to the sucrose analogue. We therefore tested the effects of

turanose on auxin accumulation. This was done by using DR5::GUS transgenic *Arabidopsis* plants bearing the DR5 synthetic promoter, highly responsive to auxin (Ulmasov *et al.*, 1997). Five-day-old control DR5 plants showed a faint blue coloration only in the root apex (Figure 3a). Conversely, 5-day-old turanose-treated DR5 plants accumulated auxin in

the root apex, root elongation zone, hypocotyl, and basal and apical parts of the cotyledons (Figure 3b), indicating that an increase in auxin content was induced by turanose. This increase preceded the formation of adventitious root primordia, not yet visible in 5-day-old hypocotyls (Figure 3b). Ten days after germination (DAG), newly formed root primordia were detected easily in hypocotyl of turanose-treated DR5 plants, showing a clear accumulation of auxin, as deduced from the strong GUS activity (Figure 3e–h), while in DR5 plants grown on control medium only the primary root apex showed auxin accumulation (Figure 3c,d).

We tested whether the *tin* mutant showed insensitivity to auxin by comparing its growth response to 2,4-D with that of the wild type and the auxin-insensitive *axr1-3* mutant. The *tin* mutant was sensitive to exogenous auxin similarly to wild-type seedlings (Figure S2a). On the other hand, the *axr1-3* mutant was not turanose-insensitive (Figure S2b). Turanose insensitivity was not observed in several other auxin mutants including *axr1-7*, *axr4-1*, *axr4-2*, *axr6-1*, *axr6-2*, *aux1-7*, *aux40*, *pid1*, *pin1-1*, *tir1-1*, *tir3-101*, and in the double mutants *aux1-7 axr4-2* and *axr1-3 axr4-2* (data not shown). These results suggest that the role of auxin in the turanose-dependent phenotype is not related to most of the known players involved in auxin signalling.

The *tin* mutation arises from a chromosomal translocation

Three different T-DNA insertions were identified in the *tin* genome. Two were found in intergenic regions of the same arm of chromosome 1, downstream of genes *At1g48730* and *At1g71870*, respectively. The third T-DNA insertion was located in chromosome 3 near the end of the second exon of gene *At3g11260*, 31 nt upstream of the stop codon (Figure 4a). In order to evaluate if the T-DNA insertions in chromosome 1 affected the genetic expression of the surrounding regions, we performed an mRNA profiling experiment using RNA extracted from the wild-type and

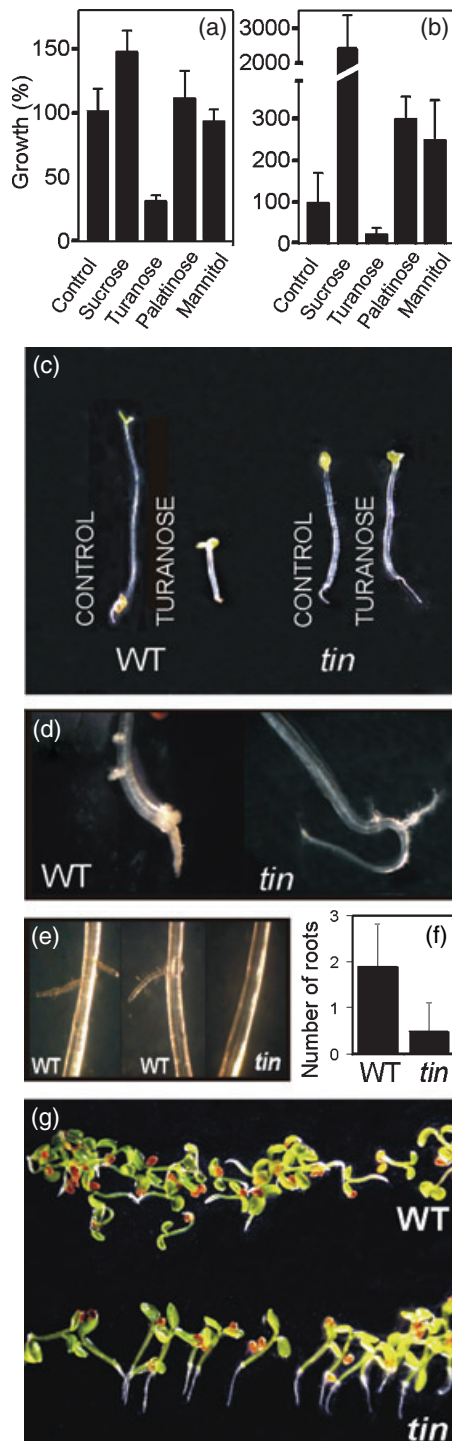


Figure 1. Effects of turanose and sucrose on seedling morphology.

(a, b) Effects of various treatments on hypocotyl (a) and root (b) growth. *Arabidopsis* seeds were germinated in the absence (control) or presence of sucrose, turanose, palatinose and mannitol (90 mM). 10 days after germination (DAG), seedlings were collected and measured using a microscope. Data are mean \pm SD ($n = 20$) and are expressed as percentages (control = 100). (c) Morphology of 5-DAG wild-type and *tin* seedlings grown in the absence (control) or presence of 90 mM turanose. (d, e) Effect of turanose (d) and sucrose (e) on adventitious root production in wild-type and *tin* mutant. *Arabidopsis* seedlings were grown in the dark on vertical plates containing 90 mM turanose (d) or 90 mM sucrose (e). Photographs were taken 10 days after the beginning of the experiment. (f) Number of adventitious roots developed in wild-type and *tin* hypocotyls grown in the dark on vertical plates containing 90 mM sucrose. Adventitious roots were counted 10 days after the beginning of the experiment. Data are mean \pm SD ($n = 20$).

(g) Gravitropic response in wild-type and *tin* seedlings grown in the light (see Experimental procedures) on vertical plates containing 90 mM turanose. Gravitropic response was evaluated by comparing the ability of wild-type and *tin* seedlings to orient hypocotyl and root according to gravity.

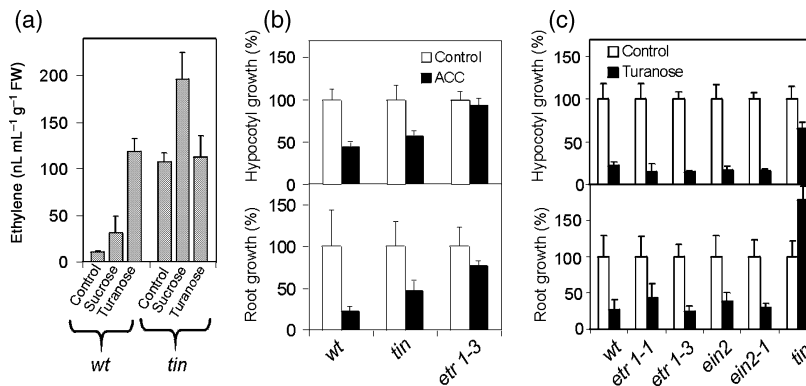


Figure 2. Role of ethylene in seedlings responses to turanose and sucrose.

(a) Ethylene production in wild-type and *tin* mutant. Seedlings were grown in sterile flasks containing $0.5 \times$ MS medium (control) supplemented with 90 mM sucrose or turanose. Flasks were sealed the day before analysis. A sample of the headspace atmosphere was collected using a syringe and ethylene was quantified as described in Experimental procedures. Data are mean \pm SD ($n = 4$).

(b) Effects of 50 μ M ACC on hypocotyl and root growth in wild-type, *tin* and ethylene-insensitive *etr1-3* mutant. At 5 DAG seedlings were collected and measured using a microscope. Data are mean \pm SD ($n = 20$) and are expressed as percentages (control = 100).

(c) Effects of 90 mM turanose on hypocotyl and root growth in wild-type, *tin* and ethylene-insensitive mutants. At 5 DAG seedlings were collected and measured using a microscope. Data are mean \pm SD ($n = 20$) and are expressed as percentages (control = 100).

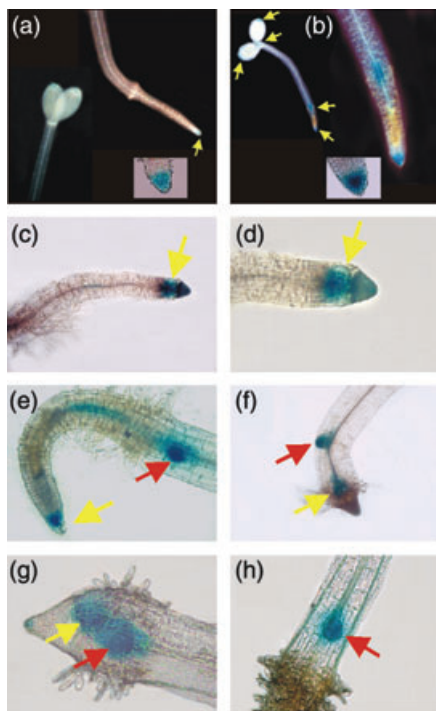


Figure 3. Auxin distribution as evaluated using DR5::GUS seedlings.

Control seedlings (a, c, d) were germinated on $0.5 \times$ MS medium and grown for 5 days (a) or 10 days (c, d). Turanose (90 mM)-treated seedlings (b, e–h) were grown for 5 days (b) or 10 days (e–h). Yellow arrows in (b) indicate regions of auxin accumulation. Arrows in (c–h) indicate primary root apex (yellow) and adventitious root apex (red).

tin seedlings and the whole-genome ATH1 Affymetrix GeneChip. None of the genes upstream or downstream of these insertions showed altered expression (Table S1). As a

consequence, the only insertion related to the phenotype observed in *tin* seedlings appeared to be that in chromosome 3. *At3g11260* is a *WUSCHEL*-related homeobox gene known as *WOX5*, expressed in the root quiescent centre (QC) (Haecker *et al.*, 2004). We found that *WOX5* was expressed at a low level in germinating seedlings, but its expression was clearly induced after an auxin treatment (Figure 4b). Interestingly, *WOX5* expression was also detected in the auxin-treated *tin* mutant, but its transcript appeared longer (Figure 4b). Cloning the mutated *WOX5* transcript (*TIN* transcript) from *tin* seedlings revealed that it corresponded to a chimeric transcript comprising the *At3g11260* coding sequence to 68 nt upstream of the stop codon, and the transcript of *At1g48610* from 6 nt upstream of the ATG codon to almost the entire 3' untranslated region (UTR) (Figure 4f). The two coding sequences are in-frame. The identification of this chimeric transcript revealed that the *tin* mutation arose from a chromosomal translocation between chromosomes 1 and 3, probably due to, or promoted by, the multiple T-DNA insertions. Major chromosomal rearrangements, including translocation events, associated with T-DNA integrations have been described (Nacry *et al.*, 1998; Ray *et al.*, 1997; Tax and Vernon, 2001). Castle *et al.* (1993) found chromosomal rearrangement events were widespread after seed transformation in *Arabidopsis*, estimating as many as approximately 17% of mutated embryos harbouring chromosomal translocations.

Isolation of the chimeric transcript allowed us to clone the chimeric gene, confirming the occurrence of a fusion event. In particular, almost the entire sequence of *At3g11260* upstream of the T-DNA insertion resulted, to be fused with a sequence that started 325 bp upstream of *At1g48610* 5' UTR. The absence of intact copies of both *At3g11260* and

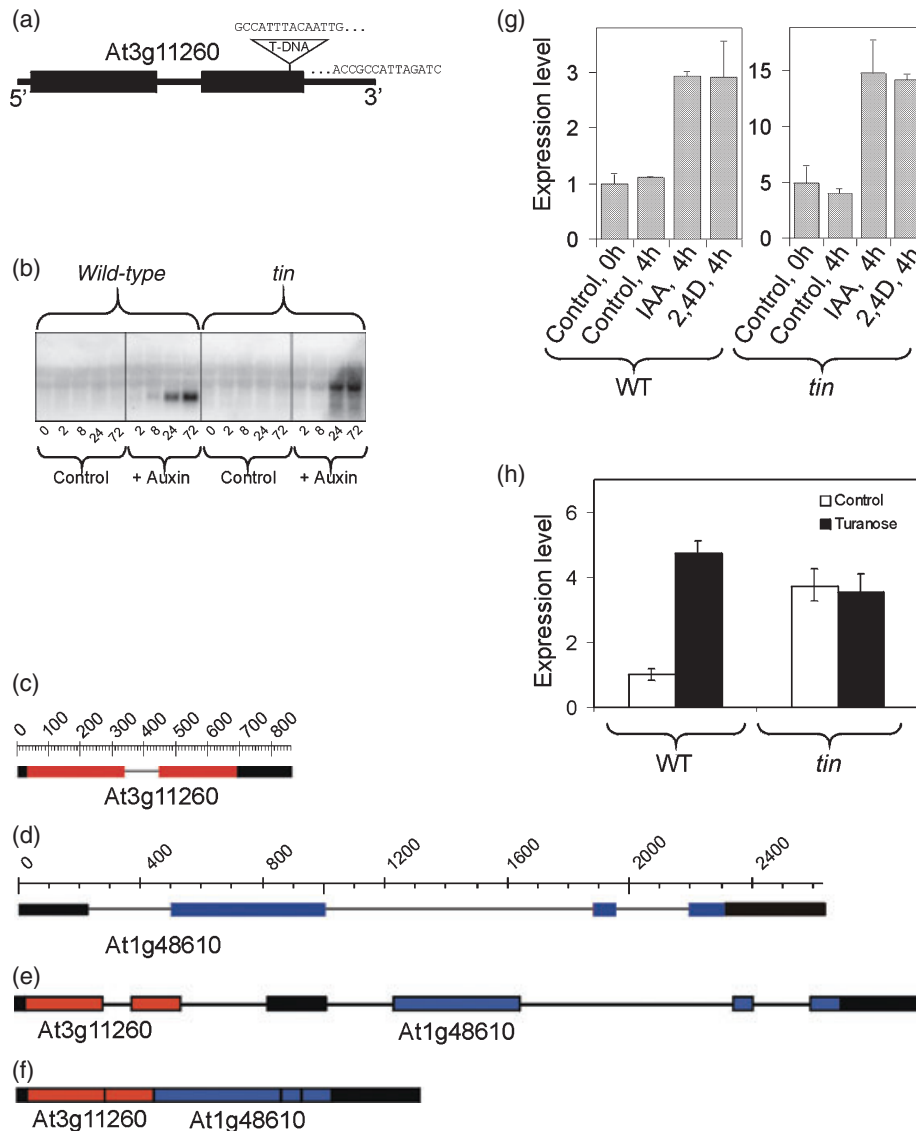


Figure 4. Structure, auxin, and turanose inducibility of *At3g11260* and its mutated form.

(a) Position of T-DNA insertion identified in chromosome 3 within *At3g11260*.

(b) Northern blot analysis of *At3g11260* expression in 3-DAG dark-grown wild-type and *tin* seedlings incubated for additional 0–72 h, as indicated, on $0.5 \times$ MS medium (control) and $20 \mu\text{M}$ 2,4-D (+auxin).

(c) Structure of wild-type *At3g11260* gene. Black thick segments, untranslated regions (UTRs); red thick segments, exons; black thin segments, introns.

(d) Structure of wild-type *At1g48610* gene. Black thick segments, UTRs; blue thick segments, exons; black thin segments, introns.

(e) Structure of *At3g11260* + *At1g48610* fusion gene identified in *tin* mutant (*TIN* gene). Black thick segments, UTRs; red thick segments, exons from *At3g11260*; blue thick segments, exons from *At1g48610*; black thin segments, introns.

(f) Structure of *At3g11260* + *At1g48610* chimeric transcript identified in *tin* mutant. Colours of segments as in (e).

(g) Real-time RT-PCR analysis of *At3g11260* expression in wild-type and *tin* seedlings grown in the dark for 5 days on MS (control, 0 h) and for an additional 4 h on MS (control, 4 h) or $20 \mu\text{M}$ IAA (IAA, 4 h) or $20 \mu\text{M}$ 2,4-D (2,4-D, 4 h). Expression levels are indicated in relative units (1 = expression in wild-type control), 0 h. Each value is mean \pm SD of three independent measurements.

(h) Real-time RT-PCR analysis of *At3g11260* expression in wild-type and *tin* seedlings grown in the dark for 3 days on MS (control) and 90 mM turanose. Expression levels are indicated in relative units, assuming as unitary the value of wild-type control. Each value is mean \pm SD of three independent measurements.

At1g48610 in the genome of the *tin* mutant was demonstrated by PCR analysis, with primers annealing up- and downstream of the fusion site in the wild-type allele of each mutated gene (data not shown). The translocation event is summarized in Figure 4(c–f), showing the *At3g11260* gene

(*WOX5*, Figure 4c); the *At1g48610* gene (Figure 4d); the chimeric gene found in the *tin* mutant (*TIN* gene, Figure 4e); and its transcript (Figure 4f). The presence of a chromosomal translocation was confirmed by segregation analysis of the T-DNA insertions. Indeed, the T-DNA insertion found in

chromosome 3 and that identified in chromosome 1 downstream of *At1g71870* did not segregate independently in the F_2 progeny from the cross between wild-type and *tin* plants (data not shown), demonstrating that they were linked, being located in the same chromosome arm after the translocation event. *WOX5* and chimeric *WOX5 (TIN)* genes were inducible by either indole acetic acid (IAA) or 2,4-D in both wild type and *tin* mutant (Figure 4g). The level of expression of chimeric *WOX5 (TIN)* on the control medium is higher than in the wild type (Figure 4g,h). Interestingly, induction by turanose was observed only in the wild type (Figure 4h).

Gene *At1g48610* has not yet been characterized. Its product is identified as an 'AT-hook motif-containing protein' (TIGR *Arabidopsis thaliana* database: <http://www.tigr.org>). The AT-hook motif is characteristic of a class of nuclear proteins interacting with chromatin and known as high-mobility group (HMG) proteins (reviewed by Klosterman and Hadwiger, 2002). *At1g48610* expression was not modulated by either turanose or auxin, and a knock-out in *At1g48610* did not phenocopy the *tin* mutation (data not shown).

Microarray comparison of the transcript profiles of wild-type and *tin* plants demonstrated that the chromosomal translocation did not affect the expression of genes along the two chromosomes involved, upstream or downstream of the T-DNA insertion within *At3g11260* (Figure S3).

Overexpression of WOX5 complements tin mutation

Although the auxin and turanose inducibility of *WOX5* gene is highly suggestive of its role in the observed response of seedlings to turanose, the complex chromosomal rearrangement observed in the *tin* mutant indicates that additional evidence is required to assess the involvement of *WOX5* in the observed phenotype. A transgenic line overexpressing the chimeric *TIN* gene ($35S::TIN$) was obtained and showed turanose insensitivity, demonstrating that the presence of the *TIN* gene is sufficient for the observed *tin* phenotype (data not shown). *WOX5* is expressed in the root QC (Haecker *et al.*, 2004), and correlates with the reduced adventitious root production in turanose-treated *tin* mutant (Figure 1d). For this reason we focused attention on its mutation. The sequence of *WOX5* within the *TIN* chimeric gene is interrupted, and the relative polypeptide should be defective in at least 30 terminal amino acids plus the entire 3' UTR corresponding region. An *Arabidopsis wox5* mutant, characterized by a transposon insertion at the end of the first exon of the *WOX5* gene, was identified but did not phenocopy the *tin* mutation, and did not present any peculiar phenotype (data not shown). *Arabidopsis* plants overexpressing the *WOX5* gene ($35S::WOX5$) did not differ from the wild type in their morphology (Figure 5a). Nevertheless, crossing this transgenic line with the *tin* mutant resulted in

complementation of the *tin* mutation, shown by the ability of the cross ($35S::WOX5/TIN$) to respond to turanose exhibiting the wild-type phenotype (Figure 5a). Statistical analysis of the effects of turanose on root length indicates that the cross ($35S::WOX5/TIN$) is as turanose-sensitive as the wild type (Figure 5b). This is of importance as the heterozygous *tin* mutant (*WOX5/TIN*) was turanose-insensitive (Figure 5a,b), although its turanose-grown root was shorter than that of the homozygous *tin* (*TIN/TIN*). The strong turanose insensitivity shown by the *tin* mutant (*TIN/TIN*) is thus somehow reduced when a single *WOX5* gene copy is present in the genome (*WOX5/TIN*), but only the overexpression of *WOX5* in a *tin* background ($35S::WOX5/TIN$) restores the wild-type root phenotype. *WOX5* can therefore complement the *tin* mutation, provided it can overcome the competition with *TIN* expression (Figure 5a,b). To evaluate whether the semi-dominant *tin* phenotype shown by the heterozygous *WOX5/TIN* plants (Figure 5a,b) is confirmed by the response to turanose in terms of auxin accumulation, we crossed the *tin* mutant with DR5::GUS transgenic *Arabidopsis* plants bearing the DR5 synthetic promoter, which are highly responsive to auxin (Ulmasov *et al.*, 1997). In the F_2 progeny we obtained *WOX5/WOX5/DR5* and *TIN/TIN/DR5* seedlings as well as heterozygous *WOX5/TIN/DR5* seedlings (see Experimental procedures), all showing a comparable response to exogenous auxin in terms of GUS staining (data not shown). When treated with turanose, *WOX5/WOX5/DR5* seedlings grown on solid incubation medium showed a strong blue staining, indicating increased auxin content, mostly restricted to the root/hypocotyl transition zone (Figure 5c, left panels, red arrows). Seedlings were stained blue in the root and most of the upper parts of the hypocotyl and cotyledons when the turanose treatment was performed using seedlings growing in a liquid incubation medium (Figure 5c, right panel), suggesting that auxin diffuses in the liquid medium, activating the DR5 promoter in most of the seedling tissues. Interestingly, the *TIN/TIN/DR5* seedlings showed only a faint blue staining, and the same was observed in heterozygous *WOX5/TIN/DR5* seedlings, indicating that the heterozygotes' behaviour mirrors that of the homozygous *tin* mutant in terms of auxin production in response to turanose (Figure 5c).

Altered auxin homeostasis in the tin mutant

The results obtained using expression patterns of the synthetic auxin reporter DR5-GUS suggest that the *tin* mutant does not accumulate auxin in response to turanose. We therefore proceeded to analyse auxin content in seedlings using gas chromatography coupled to mass spectrometry (GC-MS). Turanose-treated wild-type seedlings showed a marked increase in free IAA content, while the *tin* mutant did not display any increase in free IAA in response to turanose (Figure 6a). The level of both ester-type (Figure 6b) and

amide-type IAA conjugates (Figure 6c) is high in turanose-treated wild-type seedlings. Conversely, turanose reduced the level of ester-type (Figure 6b) and, more markedly, of amide-type bound IAA (Figure 6c) in *tin* seedlings. Turanose treatment leads to a different morphology in wild-type seedlings (Figure 1c). The higher level of IAA conjugates

(Figure 6b,c) in wild-type seedlings treated with turanose alone could be a consequence of the retarded seedling development and slower degradation of the conjugated auxin present in the seed. Wild-type seedlings treated with turanose in the presence of sucrose do not show the short root phenotype and abolish morphological differences between the wild-type and *tin*, except for the production of adventitious roots, which is not observed in *tin* (data not shown). This allows us to investigate differences between wild-type and *tin* seedlings unrelated to the effects of turanose on seedling developmental stage. Wild-type seedlings treated with turanose in the presence of sucrose show an IAA level (Figure 6d) comparable with that of seedlings treated with turanose alone (Figure 6a), indicating that turanose-triggered auxin increase is not a consequence of the different phenotype shown by turanose-treated seedlings. No increase in auxin conjugates was observed when comparing sucrose-treated seedlings with those grown in the presence of both sucrose and turanose (Figure 6e,f). While seedlings used for auxin analysis (Figure 6a–c) display strong morphological differences (Figure 1c), auxin analysis data reported in Figure 6(d–f) were obtained from seedlings at the same developmental stage (root and hypocotyl length). Therefore uncoupling the effects of turanose on wild-type seedling morphology from its role on auxin physiology reveals that turanose increases free IAA level,

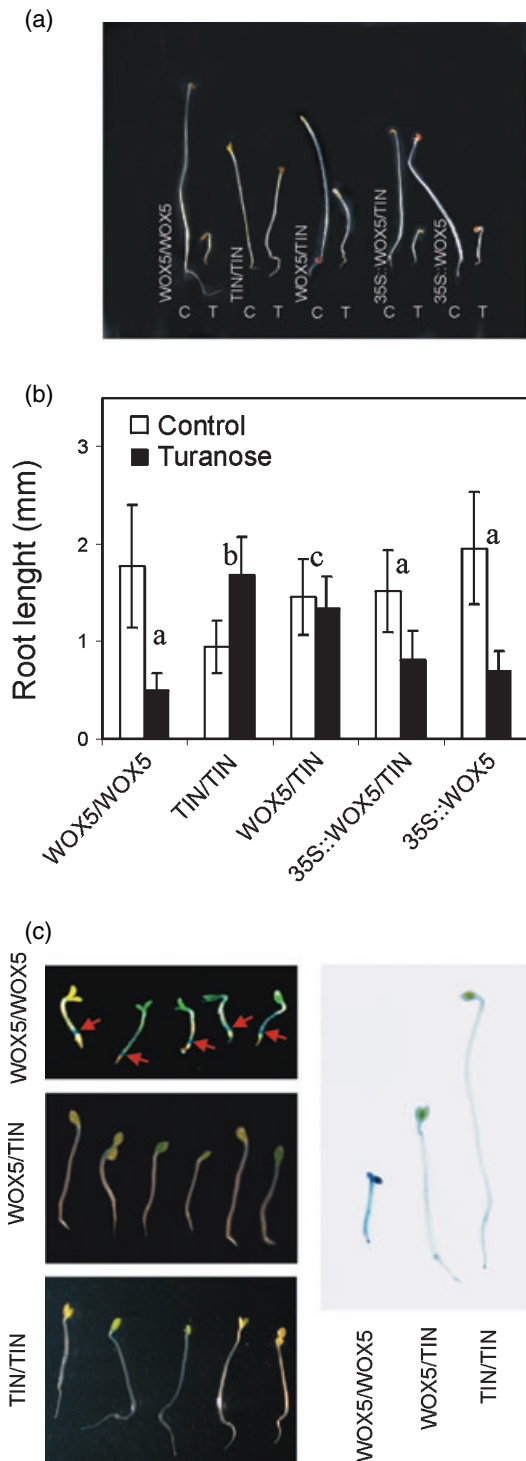


Figure 5. Complementation of *tin* mutation by overexpression of *WOX5*.

(a) Effects of turanose on seedling morphology in wild type (*WOX5/WOX5*), homozygous *tin* mutant (*TIN/TIN*), heterozygous *tin* mutant (*WOX5/TIN*), cross between *tin* and *WOX5* overexpressing transgenic (*35S::WOX5/TIN*), and *WOX5* overexpressing transgenic (*35S::WOX5*). 5-DAG seedlings grown in the dark in the absence (C, control) or presence of 90 mM turanose (T, turanose) were collected and photographed.

(b) Effects of turanose on root growth in wild type (*WOX5/WOX5*), homozygous *tin* mutant (*TIN/TIN*), heterozygous *tin* mutant (*WOX5/TIN*), cross between *tin* and *WOX5* overexpressing transgenic (*35S::WOX5/TIN*), and *WOX5* overexpressing transgenic (*35S::WOX5*). 5-DAG seedlings grown in the dark in the absence (control) or presence of 90 mM turanose were collected and measured using a microscope. Data are mean \pm SD ($n = 20$) and are expressed as percentages (control = 100). Data were analysed for statistical significance by two-way ANOVA ($\alpha = 0.0001$) with treatment (control, turanose) and genotype as class variables. Different letters indicate significant differences (treatment \times genotype) between groups.

(c) Effects of turanose on auxin accumulation in wild type (*WOX5/WOX5*), homozygous *tin* mutant (*TIN/TIN*), and heterozygous *tin* mutant (*WOX5/TIN*). To test the ability of turanose to increase auxin levels, expression patterns of the synthetic auxin reporter DR5-GUS were examined in seedlings treated with turanose (90 mM). DR5-GUS activity has been found to correlate well with endogenous auxin levels in *Arabidopsis* (Benkova *et al.*, 2003; Casimiro *et al.*, 2001). The three genotypes are in a DR5::GUS background, blue staining indicates auxin accumulation. 5-DAG seedlings grown in the dark in the presence of 90 mM turanose were collected and stained for GUS activity. Seedlings were grown in solid medium (left panels, red arrows indicate strong blue staining in the root–hypocotyl transition zone) and liquid medium (right panel). Seedlings grown in the absence of turanose showed GUS staining restricted to the root apex (data not shown). Seedlings were then photographed and subsequently extracted for DNA to identify the genotype of each single seedling. Over 20 seedlings were analysed and identified for each genotype. A representative group of seedlings is shown.

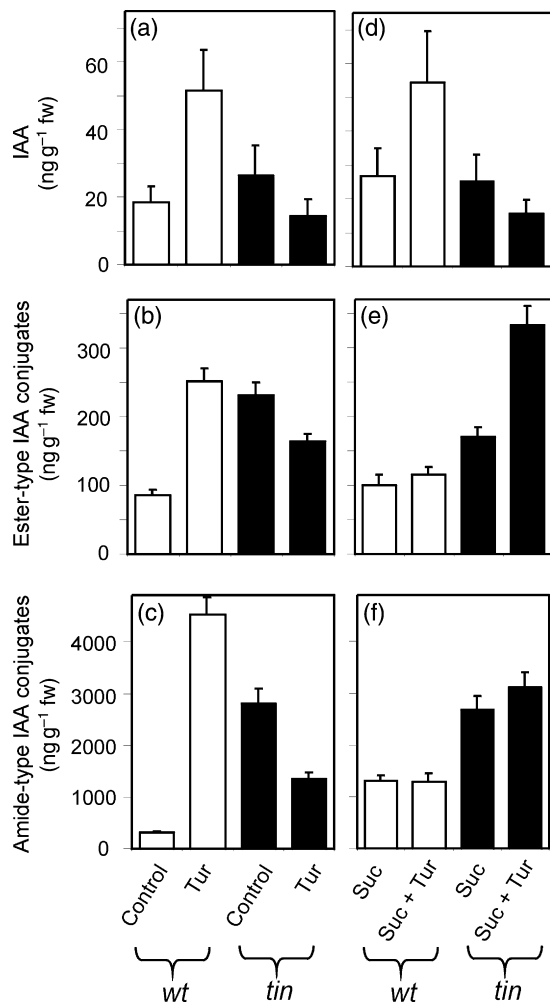


Figure 6. Auxin production in wild-type and *tin* mutant. Seedlings were grown in sterile flasks containing 0.5 × MS (control), supplemented with 90 mM sucrose, 90 mM turanose, or 15 mM sucrose + 90 mM turanose (tur + suc). 5-DAG seedlings were collected and analysed for free (a, d); ester-type conjugated IAA (b, e); and amide-type conjugated IAA (c, f).

but has no effect on IAA conjugates. Comparison of sucrose-treated *tin* seedlings with sucrose + turanose seedlings shows that the latter display a lower IAA content (Figure 6d) accompanied by a rise in ester-type conjugates (Figure 6e), suggesting an efficient IAA conjugation in *tin* challenged with turanose. Overall, not only the control *tin*, but also the sucrose-treated *tin* mutant, displays a higher IAA-conjugate level when compared with the wild type (control and sucrose-treated) (Figure 6e,f). Interestingly, plants overexpressing *WOX5* (35S::*WOX5*) displayed a reduced level of IAA conjugates when turanose-treated (60% reduction compared with wild type), while *wox5* plants showed the same level of IAA conjugates as the wild type (data not shown). The level of IAA in both 35S::*WOX5* and *wox5* was comparable with that of their respective wild types (data not shown).

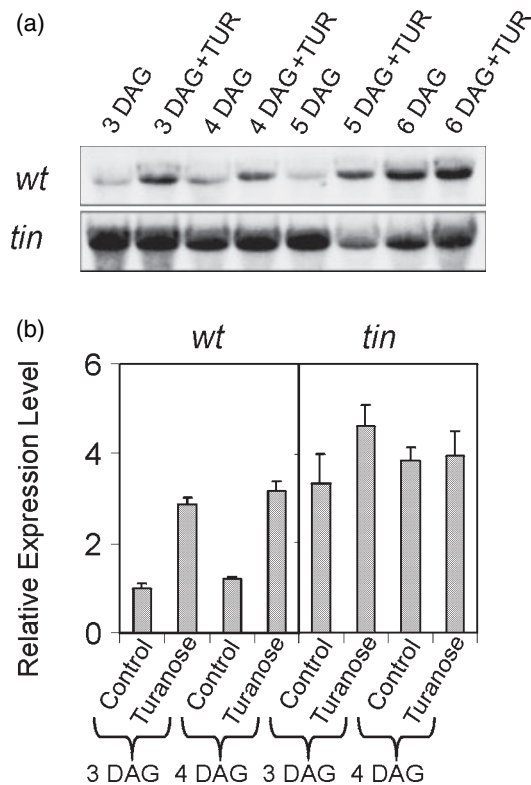


Figure 7. Analysis of *SUR2* expression in wild-type and *tin* seedlings. (a) Northern blot analysis of *SUR2* expression in 3–6-DAG wild-type and *tin* seedlings grown in the dark on MS ± 90 mM turanose. (b) Real-time RT-PCR analysis of *SUR2* expression in wild-type and *tin* seedlings grown in the dark for 3–4 days on MS in the absence (control) or presence of 90 mM turanose. Expression levels indicated in relative units assuming as unitary the value of wild-type 3-DAG control. Each value is mean ± SD of three independent measurements.

Auxin homeostasis can also be achieved by the *SUR1/SUR2* pathway (Barlier *et al.*, 2000; Mikkelsen *et al.*, 2004). We analysed *SUR1* and *SUR2* transcript levels in wild-type and *tin* seedlings. Induction of *SUR1* by turanose was observed in both wild type and *tin* mutant, without significant differences (data not shown). Expression of *SUR2* was high in turanose-treated wild-type seedlings (Figure 7a,b) as well as in sucrose-treated seedlings (data not shown). The *SUR2* mRNA level was, instead, constitutively high in *tin*, particularly in 3- and 4-DAG seedlings (Figure 7a), with a modest increase in the presence of turanose, as demonstrated by both Northern blot and real-time RT-PCR analyses (Figure 7a,b).

Discussion

The *tin* mutant expresses a chimeric form of *WOX5* gene (Figure 4), a member of the *WOX* gene family (Haecker *et al.*, 2004). Turanose insensitivity is associated with altered auxin homeostasis, as suggested by the higher levels of IAA

conjugates and *SUR2* expression (Figures 6 and 7), showing the existence of a relationship between turanose and auxin, as previously suggested for the effects of sucrose on root development (Malamy, 2005). The *tin* mutation can be complemented by overexpression of *WOX5* (Figure 5), indicating that *tin* is probably a *WOX5* loss-of-function mutant. Nevertheless, a *wox5* mutant does not phenocopy the *tin* mutation, suggesting that other genes are functionally redundant with *WOX5*. Interestingly, the *WOX5* sequence is very similar to another *WOX* gene, *WOX7* (Haecker *et al.*, 2004), and expression of the two genes could be somehow redundant. Haecker *et al.* (2004) hypothesized that genetic redundancy may exist among *WOX* genes as insertional mutants for *WOX1*, 5, 8 and 9 did not show any evident developmental defects, and only *wox2* mutants showed specific perturbations in embryonic patterning. Expression of the chimeric *WOX5 (TIN)* gene unveils clues about the physiological role of *WOX5*. The possibility that chimeric proteins can help elucidate the function of genes by forming complexes with partners of the wild-type protein, or by facilitating protein aggregation, was demonstrated for the *heat shock factor 1 (AtHSF1)* gene, which can form biologically active trimers only when overexpressed as a *HSF-GUS* or *GUS-HSF* chimeric gene (Lee *et al.*, 1995). Similarly, the chimeric *TIN* protein may interact (thus hampering their biological activity) with protein partners required for *WOX5* action as well as for the activity of its functionally redundant proteins. Kamiya *et al.* (2003) suggested that *WUSCHEL*-type homeodomain transcription proteins could form dimers.

WOX5 expression is induced by turanose (Figure 4h) as well as by auxin (Figure 4g) in wild-type seedlings. Induction by auxin of the chimeric *WOX5 (TIN)* gene can be observed in *tin* (Figure 4g), while turanose is unable to trigger increased chimeric *TIN* mRNA accumulation in the mutant (Figure 4h). As a turanose-dependent increase in auxin content is observed in the wild type but not in *tin* (Figure 6a,d), we conclude that turanose induction of *WOX5* is mediated by auxin. *WOX5* is expressed in the QC cells of the root meristem and in their direct precursor cells at the early globular embryo stage (Haecker *et al.*, 2004) as well as in the QC of the seedling root (Blilou *et al.*, 2005). A putative rice homologue of *WOX5* described previously (*quiescent centre-specific homeobox, QHB*; Kamiya *et al.*, 2003) was shown to be expressed during embryogenesis in specific cells related to root tip formation as well as in the central cells of the mature root QC. This gene was therefore proposed to be involved in the specification and maintenance of the root apical meristem (Kamiya *et al.*, 2003) with a mechanism similar to that of *WUSCHEL* in the shoot apical meristem (Laux *et al.*, 1996).

We suggest that the increased, diffuse auxin presence induced by turanose in the root and hypocotyl (Figure 3b) induces a set of genes involved in the differentiation of root

primordia, and that *WOX5* is among these genes (Figure 4g,h). The induction of *WOX5* by auxin could be responsible for the inhibition of primary root growth in wild-type seedlings on turanose, as a consequence of the development of adventitious roots. The mutation of *WOX5* in *tin* seedlings, associated with altered auxin homeostasis, leads to a slightly shorter root length in normal conditions, and to turanose insensitivity and the consequent phenotype in the presence of the disaccharide. The observed effects at the level of hypocotyl length as well as in the adult plant (delayed flowering) are probably pleiotropic effects of the mutation, possibly related to the altered hormonal metabolism observed in *tin*.

The production of adventitious roots in *Arabidopsis* is stimulated by sucrose (Takahashi *et al.*, 2003; Figure 1e) and turanose (Figure 1d) by triggering auxin accumulation in the hypocotyl (Figure 3b). The ability of auxin to induce production of lateral and adventitious roots is well known, while the mechanism behind this developmental process is still largely obscure. A graded distribution of auxin near the QC correlates with correct patterning (Friml *et al.*, 2002), and the putative auxin carrier *AtPIN4* is required for channelling auxin from the source of auxin production to the root apex (Friml *et al.*, 2002). Auxin concentration increases as a consequence of *AtPIN4* activity, which generates a sink for auxin where the 'auxin maximum' will then be established (Friml *et al.*, 2002). A recent report has demonstrated that five *PIN* genes collectively control auxin distribution in the primary root (Blilou *et al.*, 2005). In addition to transport-regulated auxin gradients in the root, local auxin synthesis and catabolism may contribute to establishing the auxin maximum near the QC cells (Ljung *et al.*, 2002, 2005). Expression of genes involved in IAA synthesis coincides with the auxin maximum observed in the root apex in the area where *WOX5* is expressed (Ljung *et al.*, 2005). Remarkably, analysis of the microarray expression data published by Birnbaum *et al.* (2003) shows a good correlation between the mRNA level of the auxin biosynthetic gene *CYP79B2* and that of *SUR2* in the root tip ($R^2 = 0.7275$), reinforcing the view that active auxin synthesis in the root apex (*CYP79B2*) is coupled with *SUR2*-dependent homeostatic control (Barlier *et al.*, 2000).

Induction of *WOX5* by turanose-induced auxin in the primary root apex and in the other root primordia of wild-type seedlings (Figure 3d,e) probably results in repression of *SUR2* (*SUR2* being constitutively expressed in *tin*, Figure 7), and in the localized repression of the auxin conjugation pathway (which is very active in *tin*, Figure 6, and less active in the 35S::*WOX5* line). Repression of *SUR2* contributes to producing the localized free IAA accumulation commonly observed in wild-type seedlings in the primary root apex as well as in the primordia of lateral and adventitious roots. The importance of this pathway as a homeostatic mechanism to control free IAA levels is clearly

evident in *sur1* and *sur2* mutants (Barlier *et al.*, 2000; Mikkelsen *et al.*, 2004).

A local increase in auxin concentration is associated with the development of new root primordia. The area of auxin accumulation includes the QC in the primary root tip (Blilou *et al.*, 2005), and probably the same happens in adventitious and lateral root primordia where new QCs are establishing. *WOX5* is auxin-inducible (Figure 4b,g), and its expression in the QC is probably the consequence of the high auxin content near these cells. We propose that the auxin maximum in each root tip is reached step by step, by the action of PIN proteins generating an influx of auxin (Blilou *et al.*, 2005) that induces *WOX5*, which, in turn, allows maintenance of the auxin maximum by repression of IAA conjugation as well as by favouring *in situ* auxin synthesis (Ljung *et al.*, 2005) through inhibition of the SUR2 pathway. *WOX5* could therefore play a role in contributing to maintaining QC identity, as far as auxin level is concerned, by the repression of homeostatic mechanisms that would hamper establishment of the highest auxin concentration in this localized area of the root apex.

Experimental procedures

Plant material and growth conditions

Arabidopsis thaliana ecotype Columbia glabra (gl1-1) was used in this study. Seeds were sterilized with diluted bleach (10 min incubation in 1.7% v/v sodium hypochlorite, rinsing and washing thoroughly in sterile water) and germinated in petri dishes. Horizontal and vertical plates were prepared using solid growing media (MS half-strength solution containing 1% agar and turanose or sucrose at concentrations reported in figure legends). Seeds were germinated in the dark in most experiments, with the exception of the gravitropism test (Figure 1g) which was performed using seedlings grown under a 14/10-h photoperiod at 150 $\mu\text{mol photons m}^{-2} \text{sec}^{-1}$. When added, sucrose or turanose was present throughout the experiment. Seeds were germinated in liquid medium for hormone quantification, RNA extraction and microarray experiments.

The *wox5* mutant, corresponding to the genetrap line GT11084, was obtained from the Martienssen Laboratory (<http://genetrap.cshl.org>) at Cold Spring Harbor Laboratory.

GUS staining

GUS staining was performed following the protocol reported by Jefferson (1987). Seedlings were collected and incubated at 37°C for 4 h in a solution of 5-bromo-4-chloro-3-indolyl glucuronide (X-gluc). X-gluc solution was prepared by dissolving 5 mg X-gluc in 50 μl dimethylformamide, then added to 5 ml 50 mM NaPO_4 pH 7.0. After staining, seedlings were incubated in 70% ethanol and observed under a light microscope.

Mutant selection

Screening of insertional mutants was carried out in petri dishes containing 0.5 \times MS, 1% agar and 90 mM turanose, using 630

different T-DNA tagged lines belonging to the Jack T-DNA enhancer trap lines collection (Campisi *et al.*, 1999). These lines were obtained from the Nottingham Arabidopsis Stock Centre (Scholl *et al.*, 2000). Seedlings were observed under a microscope at 5 DAG to search for seedlings showing normal hypocotyl and root development. Putative turanose-insensitive mutants were collected, transferred to petri dishes containing 0.5 \times MS, 1% agar and 90 mM sucrose in the light for 15 days (14/10-h photoperiod at 150 $\mu\text{mol photons m}^{-2} \text{sec}^{-1}$) to allow safe transfer to soil. Seeds collected from putative resistant mutants were rescreened on turanose to confirm the phenotype. The *tin* mutant described here was isolated within pool no. 19678.

Molecular characterization of tin

DNA extraction was performed with the GenElute Plant Genomic DNA Miniprep Kit (Sigma-Aldrich, St Louis, MO, USA) using approximately 100 mg rosette leaves from 4-week-old *tin* plants. All PCR amplifications were carried out with 20 ng genomic DNA and PCR Master Mix (Promega, Madison, WI, USA). For amplification of the T-DNA/plant genome junctions, thermal asymmetric interlaced-PCR was used, as described by Liu *et al.* (1995). Primers used were AD1, AD2, AD3 and different TR1, TR2 and TR3 oligos for T-DNA left border (LB) or right border (RB). All primer sequences are reported in Table S2. The *TIN* chimeric transcript was amplified starting from poly(A)+ RNA purified by Oligotex (Qiagen, Valencia, CA, USA) from total RNA extracted from 10-day-old seedlings grown in liquid culture. RNA extraction was carried out using the aurintricarboxylic acid method as described previously (Perata *et al.*, 1997). Approximately 150 ng purified poly(A)+ RNA was subjected to a 3' RACE using the 5'/3' RACE Kit (Roche Molecular Biochemicals, Mannheim, Germany) according to the manufacturer's protocol. An oligo(dT) anchor primer in the first PCR amplification; a PCR anchor primer; and a specific *At3g11260* forward primer (A1) in the second PCR amplification were used (Table S2). The *TIN* fusion gene was amplified from genomic DNA with the primers B1 and B2 (Table S2).

Screening of tin seedlings in a DR5::GUS background

Heterozygous *WOX5/TIN* plants in a DR5 background were identified by screening seeds collected from siliques obtained from emasculated flowers of *tin* plants manually crossed with DR5::GUS pollen. Heterozygous *WOX5/TIN* plants in a DR5 background were selfed, and the resulting homozygous *TIN/TIN* and *WOX5/WOX5* plants in a DR5 background were identified and their seeds harvested and used for the experiments. Heterozygous *WOX5/TIN* seeds in a DR5 background were obtained similarly from the progeny of heterozygous *WOX5/TIN* plants bearing the DR5::GUS construct. Seeds were surface sterilized as described, and germinated in petri dishes both in liquid and solid 0.5 \times MS medium \pm 90 mM turanose. Seedlings were collected at 5 DAG and GUS stained as described. After GUS staining each single seedling was collected, rinsed with water, and all used for DNA extraction followed by PCR amplification for genotyping. These were performed using the Extract-N-Amp Plant PCR Kit (Sigma) following the manufacturer's instructions. Primers used were B3 and B4 for the *WOX5* wild-type gene (annealing around the T-DNA insertion site within the *WOX5* gene found in the *tin* mutant), and A2 and TR1 for T-DNA insertion within the *WOX5* gene (TR1 anneal in the LB of T-DNA and A2 in the final region of *WOX5* gene downstream of T-DNA insertion). All primer sequences are reported in Table S2.

Northern blot probe design and preparation

PCR primers (Table S2) were designed to amplify the most specific region inside the gene *At4g31500* (*SUR2*) and the full-length cDNA of the gene *At3g11260* (*WOX5*). Primers used for *SUR2* were *SUR2f* and *SUR2r*. Primers used for *WOX5* were A1 and A2. Poly(A)⁺ RNA was purified, following the same procedure as described, from total RNA extracted from 10-day-old seedlings grown in liquid culture. Approximately 150 ng poly(A)⁺ RNA was reverse transcribed with random primers by Improm-II (Promega). PCR amplification was performed using 15 ng cDNA.

Real-time RT-PCR

RNA was extracted from seedlings (100 mg initial weight) grown on 0.5 × MS solution (control) or in the same medium supplemented with 90 mM turanose or 20 μM 2,4-D or IAA. Total RNA, extracted with the RNAqueous Kit (Ambion, Austin, Texas, USA) according to the manufacturer's instructions, was subjected to a DNase treatment using the TURBO DNase I Kit (Ambion). Each sample (2 μg) was reverse transcribed into cDNA with the High-capacity cDNA Archive Kit (Applied Biosystems, Foster City, CA, USA). Real-time PCR amplification was carried out with the ABI Prism 7000 Sequence Detection System (Applied Biosystems) using primers C1 and C2 for *At3g11260* (*WOX5*); D1 and D2 for *At4g31500* (*SUR2*); and UQ1 and UQ2 for the *ubiquitin10* gene (*UBQ10*). Primer sequences are reported in Table S2. *UBQ10* was used as an endogenous control. Taqman probes specific for each gene were used. Probe sequences are reported in Table S2. PCR reactions were carried out using 50 ng cDNA and TaqMan Universal PCR Master Mix (Applied Biosystems) following the manufacturer's protocol. Relative quantification of each single-gene expression was performed using the comparative C_T method as described in the ABI Prism 7700 Sequence Detection System User Bulletin No. 2 (Applied Biosystems).

Construction of 35S::WOX5 and 35S::TIN cassettes

Both full-length *WOX5* and *TIN* transcripts were amplified by one-step RT-PCR using the Titan One Tube RT-PCR Kit (Roche). Poly(A)⁺ RNA was purified, following the procedure described, from total RNA extracted from 10-day-old wild-type and *tin* seedlings grown in liquid culture. Forward and reverse primers able to insert, respectively, *KpnI* and *BamHI* restriction sites at the end of the cDNA were used: F_1 and F_2 for *WOX5*, F_1 and G_2 for *TIN* transcript (Table S2). Each transcript was then ligated in a pBIN19 derivative binary vector containing an expression cassette (p35S + NOS terminator) inserted between the *Clal* and *EcoRI* restriction sites. cDNAs were inserted exploiting a *KpnI* restriction site downstream of p35S and a *BamHI* restriction site upstream of tNOS. The resulting binary vectors were named pBINWOX5 and pBINTC, respectively.

Plant transformation

The pBINWOX5 and pBINTC constructs were mobilized into *Agrobacterium tumefaciens* GV3101 pM90Ti and then introduced into *Arabidopsis* ecotype Columbia gl1-1 using the floral dip transformation method (Clough and Bent, 1998). Plants were grown at 23°C with a 14/10-h photoperiod at 150 μmol photons m⁻² sec⁻¹. Several independent transgenic lines were analysed in the T_2 generation, and one representative line for each transformant type was chosen for subsequent analyses.

RNA isolation and gel blots

RNA extraction was performed using the aurintricarboxylic acid method as described previously (Perata *et al.*, 1997). Total RNA (20 μg) was electrophoresed on 1% (w/v) agarose glyoxal gel, and blotted onto nylon membrane (BrightStar-Plus; Ambion) using the manufacturer's suggested procedure. Membranes were prehybridized and hybridized using the NorthernMax-Gly kit (Ambion). Radiolabelled probes were prepared from gel-purified cDNAs by random primer labelling (Takara Chemicals, Shiga, Japan) with [α -³²P]-dCTP. Equal loading was checked by reprobing with an rRNA cDNA probe (not shown). RNA blots were scanned using a Cyclone Phosphoimager (Packard Bioscience, Perkin Elmer, Foster City, CA, USA).

Affymetrix GeneChips analysis

Total RNA was extracted from seedling samples using the RNAqueous kit (Ambion). RNA was processed for use on Affymetrix *Arabidopsis* ATH1 GeneChip arrays as described previously (Loreti *et al.*, 2005). Expression analysis via the Affymetrix MICROARRAY SUITE software (MAS ver. 5.0) (Affymetrix Inc., Santa Clara, CA, USA) was performed with standard parameters. Two independent, replicated experiments were performed for each experimental condition, and the output of Affymetrix MAS for each independent experiment was subjected to further analyses using EXCEL (Microsoft, Redmond, WA, USA). Signal values (indicating the relative abundance of a particular transcript) and detection call values (indicating the probability that a particular transcript is present) were generated by Affymetrix MAS. Differences in transcript abundance, expressed as signal log ratio, were calculated using the MAS change algorithm.

Auxin analysis

Free and conjugated IAA extraction and HPLC analysis were performed as described previously (Picciarelli *et al.*, 2001). GC-MS analysis was performed with a Saturn 2200 mass spectrometer coupled with a gas chromatograph (Varian, Palo Alto, CA, USA), equipped with a fused silica capillary column (Mega 5MS, 0.32 mm i.d. × 25 m). The injector temperature was settled at 250°C and the flow rate of the carrier gas (helium) was at 1 ml min⁻¹. Oven temperature was maintained at 80°C for 2 min, increased to 190°C at the rate of 30°C min⁻¹. Mass spectra were obtained by electron impact with an electron energy of 70 eV, ion source temperature at 200°C and capillary interface temperature at 250°C. A full scan was performed for identification of IAA, with a scanning mass range m/z 150–350 and a scan time of 0.5 sec⁻¹. The following most abundant ions were monitored for IAA quantification: unlabelled m/z 202 and ¹³C-labelled m/z 208. Synthesized IAA was estimated by comparing the ratio of m/z 202/203 found in the sample with the normal ratio of m/z 202/203 observed in the IAA standard. Data for each sample are means of three replicates ±SD.

Ethylene measurement

Arabidopsis seedlings were cultured in 30-ml glass bottles (Pyrex, France) with whole plastic screw caps supplied with caoutchouc rubber septa, each containing 2.5 ml medium. For ethylene determination, the containers were sealed from the beginning of the experiments and gas samples analysed at 5 DAG. Samples of 2 ml were withdrawn with hypodermic syringe and injected into an HP 5890 gas chromatograph equipped with a flame ionization detector

and a metal column (1.5 × 4 mm o.d.) packed with HaysSep T (80/100 mesh). Column and detector temperatures were 70 and 350°C, respectively. Nitrogen was used as a carrier at a flow rate of 30 ml min⁻¹. The ethylene concentration in each culture container was expressed as pl l⁻¹. Abiotic and biotic ethylene were estimated according to Mensuali-Sodi *et al.* (1992) by quantifying ethylene losses and the various contributions to ethylene accumulation in the culture system.

Acknowledgements

We wish to thank Dr T.J. Guilfoyle for kindly providing us with the DR5::GUS line, Dr J. Sheen for the *HXK* transgenic lines, and Dr S. Smeeckens for providing us with the *mig7* seeds. We also acknowledge Dr Antonietta Santaniello for help in the flowering-time experiments and Mrs Angela Teani for production of 35S::*TIN* overexpressing plants.

Supplementary Material

The following supplementary material is available for this article online:

Figure S1. Effects of turanose on seedling morphology in mutants with altered starch metabolism and sugar sensing ability.

(a) Effects of turanose (■) on hypocotyl and root growth in mutants with affected starch physiology. At 5 DAG, seedlings were collected and measured using a microscope. Both wild-type and *tin* mutant were included as controls. The starch-less *adg1-1* mutant (lacking the small ADP-Glc pyrophosphorylase subunit) shows insensitivity to trehalose (Fritzius *et al.*, *Plant Physiol.* **126**, 883–889, 2001), but we ruled out a possible turanose effect related to starch synthesis as turanose sensitivity was displayed by starch-less mutants such as *pgm* (Caspar *et al.*, *Plant Physiol.* **79**, 11–17, 1985) and *adg1-1* mutants (Lin *et al.*, *Plant Physiol.* **86**, 1131–1135, 1988) as well as by the *sex1-1* mutant (starch excess, Yu *et al.*, *Plant Cell*, **13**, 1907–1918, 2001).

(b) Effects of turanose (■) on hypocotyl and root growth in mutants and transgenics with affected sugar-sensing ability. At 5 DAG seedlings were collected and measured using a microscope. Data are mean ± SD (*n* = 20) and are expressed as percentages (control = 100). Both wild-type Columbia *gl1-1* (Col) and *tin* mutant were included as controls. Turanose may alter source–sink relations leading to altered sugar status, possibly sensed by hexokinase (Jang *et al.*, *Plant Cell*, **9**, 5–19, 1997). Four transgenic lines with altered hexokinase expression (Jang *et al.*, *Plant Cell*, **9**, 5–19, 1997) and two different sugar-sensing mutants (*gin1* is a glucose-insensitive mutant, Zhou *et al.*, *Proc. Natl Acad. Sci. USA*, **95**, 10294–10299, 1998; *mig7* is a mannose-insensitive germination mutant lacking fructokinase activity, Pego *et al.*, *Plant Physiol.* **119**, 1017–1023, 1999; Pego and Smeeckens, *Trends Plant Sci.* **5**, 531–536, 2000), as well as wild-type Wassilewskija (WS), background of *mig7*; and Bensheim (Ben), background of hexokinase transgenics, were tested: none showed insensitivity to turanose.

Figure S2. Effects of 2,4D and turanose on seedling morphology in the *axr1-3* mutant.

(a) Effects of different concentrations of 2,4-D (10⁻¹⁰ to 10⁻⁴ M) on hypocotyl and root growth in wild-type, *tin* and the auxin-insensitive *axr1-3* mutant. At 5 DAG seedlings were collected and measured using a microscope. Data are mean ± SD (*n* = 20) and are expressed as percentages (control = 100).

(b) Effects of different concentrations of turanose on hypocotyl and root growth in wild-type, *tin* and the auxin-insensitive *axr1-3* mutant. At 5 DAG seedlings were collected and measured using a

microscope. Data are mean ± SD (*n* = 20) and are expressed as percentages (control = 100).

Figure S3. Transcriptomic analysis along the two chromosomes involved in the translocation.

(a, b) Expression profile of chromosome 1 genes up- and downstream of the 1–3 chromosomal translocation present in the *tin* mutant (arrow). Blue profile, wild type (all genes on chromosome 1); red profile, *tin* mutant (genes with AGI codes lower than *At1g48610* located on chromosome 1; those with codes higher than *At1g48610* on the chromosome segment translocated on chromosome 3). Profiles in (a) and (b) are from different biological replicates.

(c, d) Expression profile of chromosome 3 genes up- and downstream of the 1–3 chromosomal translocation occurred in the *tin* mutant (arrow). Blue profile, wild type (all genes on chromosome 3); red profile, *tin* mutant (genes with AGI codes higher than *At3g11260* located on chromosome 3; those with codes lower than *At3g11260* on the chromosome segment translocated on chromosome 1). Profiles in (c) and (d) are from different biological replicates.

Table S1 Online Excel file

Table S2 List of all the primers and probes used in PCR experiments. This material is available as part of the online article from <http://www.blackwell-synergy.com>

References

- Barlier, I., Kowalczyk, M., Marchant, A., Ljung, K., Bhalerao, R., Bennett, M., Sandberg, G. and Bellini, C. (2000) The *SUR2* gene of *Arabidopsis thaliana* encodes the cytochrome P450CYP83B1, a modulator of auxin homeostasis. *Proc. Natl Acad. Sci. USA*, **97**, 14819–14824.
- Benkova, E., Michniewicz, M., Sauer, M., Teichmann, T., Seifertova, D., Jurgens, G. and Friml, J. (2003) Local, efflux-dependent auxin gradients as a common module for plant organ formation. *Cell*, **115**, 591–602.
- Birnbaum, K., Shasha, D.E., Wang, J.Y., Jung, J.W., Lambert, G.M., Galbraith, D.W. and Benfey, P.N. (2003) A gene expression map of the *Arabidopsis* root. *Science*, **302**, 1956–1960.
- Bliou, I., Xu, J., Wildwater, M., Willemssen, V., Paponov, I., Friml, J., Heidstra, R., Aida, M., Palme, K. and Scheres, B. (2005) The PIN auxin efflux facilitator network controls growth and patterning in *Arabidopsis* roots. *Nature*, **433**, 39–44.
- Boerjan, W., Cervera, M.T., Delarue, M., Beekman, T., Dewitte, W., Bellini, C., Caboche, M., Van Onckelen, H., Van Montagu, M. and Inzé, D. (1995) *Superroot*, a recessive mutation in *Arabidopsis*, confers auxin overproduction. *Plant Cell*, **7**, 1405–1419.
- Campisi, L., Yi, Y., Heilig, E., Herman, B., Cassista, A.J., Allen, D.W., Xiang, H. and Jack, T. (1999) Generation of enhancer trap lines in *Arabidopsis* and characterization of expression patterns in the inflorescence. *Plant J.* **17**, 699–707.
- Casimiro, I., Marchant, A., Bhalerao, R.P. *et al.* (2001) Auxin transport promotes *Arabidopsis* lateral root initiation. *Plant Cell*, **13**, 843–852.
- Casimiro, I., Beekman, T., Graham, N., Bhalerao, R., Zhang, H.M., Casero, P., Sandberg, G. and Bennett, M.J. (2003) Dissecting *Arabidopsis* lateral root development. *Trends Plant Sci.* **8**, 165–171.
- Casson, S.A. and Lindsey, K. (2003) Genes and signalling in root development. *New Phytol.* **158**, 11–38.
- Castle, L.A., Errampalli, D., Atherton, T.L., Franzmann, L.H., Yoon, E.S. and Meinke, D.W. (1993) Genetic and molecular characterization of embryonic mutants identified following seed transformation in *Arabidopsis*. *Mol. Gen. Genet.* **241**, 504–514.
- Chandran, D., Reinders, A. and Ward, J.M. (2003) Substrate specificity of the *Arabidopsis thaliana* sucrose transporter AtSUC2. *J. Biol. Chem.* **278**, 44320–44325.

- Clough, S.J. and Bent, A.F.** (1998) Floral dip: a simplified method for *Agrobacterium*-mediated transformation of *Arabidopsis thaliana*. *Plant J.* **16**, 735–743.
- Delarue, M., Prinsen, E., Onckelen, H.V., Caboche, M. and Bellini, C.** (1998) *Sur2* mutations of *Arabidopsis thaliana* define a new locus involved in the control of auxin homeostasis. *Plant J.* **14**, 603–611.
- Fernie, A.R., Roessner, U. and Geigenberger, P.** (2001) The sucrose analog palatinose leads to a stimulation of sucrose degradation and starch synthesis when supplied to discs of growing potato tubers. *Plant Physiol.* **125**, 1967–1977.
- Friml, J., Benkova, E., Blilou, I. et al.** (2002) AtPIN4 mediates sink-driven auxin gradients and root patterning in *Arabidopsis*. *Cell*, **108**, 661–673.
- Gibson, S.I.** (2005) Control of plant development and gene expression by sugar signaling. *Curr. Opin. Plant Biol.* **8**, 93–102.
- Haecker, A., Gross-Hardt, R., Geiges, B., Sarkar, A., Breuninger, H., Herrmann, M. and Laux, T.** (2004) Expression dynamics of *WOX* genes mark cell fate decisions during early embryonic patterning in *Arabidopsis thaliana*. *Development*, **131**, 657–668.
- Horiguchi, G., Kodama, H. and Iba, K.** (2003) Mutations in a gene for plastid ribosomal protein S6-like protein reveal a novel developmental process required for the correct organization of lateral root meristem in *Arabidopsis*. *Plant J.* **33**, 521–529.
- Jang, J.C., Leon, P., Zhou, L. and Sheen, J.** (1997) Hexokinase as a sugar sensor in higher plants. *Plant Cell*, **9**, 5–19.
- Jefferson, R.A.** (1987) Assaying chimeric genes in plants: the GUS gene fusion system. *Plant Mol. Biol. Rep.* **5**, 387–405.
- Kamiya, N., Nagasaki, H., Morikami, A., Sato, Y. and Matsuoka, M.** (2003) Isolation and characterization of a rice *WUSCHEL*-type homeobox gene that is specifically expressed in the central cells of a quiescent center in the root apical meristem. *Plant J.* **35**, 429–441.
- Klosterman, S.J. and Hadwiger, L.A.** (2002) Plant HMG proteins bearing the AT-hook motif. *Plant Sci.* **162**, 855–866.
- Koch, K.** (2004) Sucrose metabolism: regulatory mechanisms and pivotal roles in sugar sensing and plant development. *Curr. Opin. Plant Biol.* **7**, 235–246.
- Laux, T., Mayer, K.F.X., Berger, J. and Jurgens, G.** (1996) The *WUSCHEL* gene is required for shoot and floral meristem integrity in *Arabidopsis*. *Development*, **122**, 87–96.
- Lee, J.H., Hubel, A. and Schoffl, F.** (1995) Derepression of the activity of genetically-engineered heat-shock factor causes constitutive synthesis of heat-shock proteins and increased thermotolerance in transgenic *Arabidopsis*. *Plant J.* **8**, 603–612.
- Li, Z.S., Noubhani, A.M., Bourbonloux, A. and Delrot, S.** (1994) Affinity purification of sucrose binding proteins from the plant plasma membrane. *Biochim. Biophys. Acta*, **1219**, 389–397.
- Liu, Y.G., Mitsukawa, N., Oosumi, T. and Whittier, R.F.** (1995) Efficient isolation and mapping of *Arabidopsis thaliana* T-DNA insert junctions by thermal asymmetric interlaced PCR. *Plant J.* **8**, 457–463.
- Ljung, K., Hull, A.K., Kowalczyk, M., Marchant, A., Celenza, J., Cohen, J.D. and Sandberg, G.** (2002) Biosynthesis, conjugation, catabolism and homeostasis of indole-3-acetic acid in *Arabidopsis thaliana*. *Plant Mol. Biol.* **50**, 309–332.
- Ljung, K., Hull, A.K., Celenza, J., Yamada, M., Estelle, M., Normanly, J. and Sandberg, G.** (2005) Sites and regulation of auxin biosynthesis in *Arabidopsis* roots. *Plant Cell*, **17**, 1090–1104.
- Loreti, E., Alpi, A. and Perata, P.** (2000) Glucose and disaccharide-sensing mechanisms modulate the expression of alpha-amylase in barley embryos. *Plant Physiol.* **123**, 939–948.
- Loreti, E., Poggi, A., Novi, G., Alpi, A. and Perata, P.** (2005) A genome-wide analysis of the effects of sucrose on gene expression in *Arabidopsis* seedlings under anoxia. *Plant Physiol.* **137**, 1130–1138.
- Malamy, J.E.** (2005) Intrinsic and environmental response pathways that regulate root system architecture. *Plant Cell Environ.* **28**, 67–77.
- Malamy, J.E. and Ryan, K.S.** (2001) Environmental regulation of lateral root initiation in *Arabidopsis*. *Plant Physiol.* **127**, 899–909.
- M'Batchi, B. and Delrot, S.** (1988) Stimulation of sugar exit from leaf tissues of *Vicia faba* L. *Planta*, **174**, 340–348.
- Mensuali-Sodi, A., Panizza, M. and Tognoni, F.** (1992) Quantification of ethylene losses in different container-seal system and comparison of biotic and abiotic contribution to ethylene accumulation in cultured tissues. *Physiol. Plant.* **84**, 472–476.
- Mikkelsen, M.D., Naur, P. and Halkier, B.A.** (2004) *Arabidopsis* mutants in the C-S lyase of glucosinolate biosynthesis establish a critical role for indole-3-acetaldoxime in auxin homeostasis. *Plant J.* **37**, 770–777.
- Nacry, P., Camilleri, C., Courtial, B., Caboche, M. and Bouchez, D.** (1998) Major chromosomal rearrangements induced by T-DNA transformation in *Arabidopsis*. *Genetics*, **149**, 641–650.
- Perata, P., Matsukura, C., Vernieri, P. and Yamaguchi, J.** (1997) Sugar repression of a gibberellin-dependent signaling pathway in barley embryos. *Plant Cell*, **9**, 2197–2208.
- Picciarelli, P., Ceccarelli, N., Paolicchi, F. and Calistri, G.** (2001) Endogenous auxins and embryogenesis in *Phaseolus coccineus*. *Aust. J. Plant Physiol.* **28**, 73–78.
- Ray, S., Park, S.-S. and Ray, A.** (1997) Pollen tube guidance by the female gametophyte. *Development*, **124**, 2489–2498.
- Schmitt, M.R., Hitz, W.D., Lin, W. and Giaquinta, R.T.** (1984) Sugar transport into protoplasts isolated from developing soybean cotyledons. II Sucrose transport kinetics, selectivity, and modeling studies. *Plant Physiol.* **75**, 941–946.
- Scholl, R.L., May, S.T. and Ware, D.H.** (2000) Seed and molecular resources for *Arabidopsis*. *Plant Physiol.* **124**, 1477–1480.
- Sinha, A.K., Hofmann, M.G., Romer, U., Kockenberger, W., Elling, L. and Roitsch, T.** (2002) Metabolizable and non-metabolizable sugars activate different signal transduction pathways in tomato. *Plant Physiol.* **128**, 1480–1489.
- Takahashi, F., Sato-Nara, K., Kobayashi, K., Suzuki, M. and Suzuki, H.** (2003) Sugar-induced adventitious roots in *Arabidopsis* seedlings. *J. Plant Res.* **116**, 83–91.
- Tax, F.E. and Vernon, D.M.** (2001) T-DNA-associated duplication/translocations in *Arabidopsis*. Implications for mutant analysis and functional genomics. *Plant Physiol.* **126**, 1527–1538.
- Ulmasov, T., Murrett, J., Hagen, G. and Guilfoyle, T.J.** (1997) Aux/IAA proteins repress expression of reporter genes containing natural and highly active synthetic auxin response elements. *Plant Cell*, **9**, 1963–1971.
- Vanneste, S., Maes, L., De Smet, I., Himanen, K., Naudts, M., Inzé, D. and Beekman, T.** (2005) Auxin regulation of cell cycle and its role during lateral root initiation. *Physiol. Plant.* **123**, 139–146.
- Wingler, A., Fritzius, T., Wiemken, A., Boller, T. and Aeschbacher, R.A.** (2000) Trehalose induces the ADP-glucose pyrophosphorylase gene, *ApL3*, and starch synthesis in *Arabidopsis*. *Plant Physiol.* **124**, 105–114.